IOP Publishing | Institute of Physics and Engineering in Medicine Physiological Measurement

Physiol. Meas. **37** (2016) 1004–1023 doi:10.1088/0967-3334/37/7/1004

Ischemia detection from morphological QRS angle changes

Daniel Romero[1], **Juan Pablo Martínez**[2,3,4], **Pablo Laguna**[2,3,4] **and Esther Pueyo**[2,3,4]

[1] Laboratoire du Traitement du Signal et de l'Image (LTSI), Rennes, France
[2] CIBER de Bioingeniería, Biomateriales y Nanomedicina, Zaragoza, Spain
[3] BSICoS Group, I3A, University of Zaragoza, Zaragoza, Spain
[4] IIS Aragón, University of Zaragoza, Spain

E-mail: daniel.romero@univ-rennes1.fr

Received 11 January 2016, revised 5 March 2016
Accepted for publication 22 March 2016
Published 31 May 2016

Abstract

In this paper, an ischemia detector is presented based on the analysis of QRS-derived angles. The detector has been developed by modeling ischemic effects on the QRS angles as a gradual change with a certain transition time and assuming a Laplacian additive modeling error contaminating the angle series. Both standard and non-standard leads were used for analysis. Non-standard leads were obtained by applying the PCA technique over specific lead subsets to represent different potential locations of the ischemic zone. The performance of the proposed detector was tested over a population of 79 patients undergoing percutaneous coronary intervention in one of the major coronary arteries (LAD ($n = 25$), RCA ($n = 16$) and LCX ($n = 38$)). The best detection performance, obtained for standard ECG leads, was achieved in the LAD group with values of sensitivity and specificity of $Se = 90.9\%$, $Sp = 95.4\%$, followed by the RCA group with $Se = 88.9\%$, $Sp = 94.4$ and the LCX group with $Se = 86.1\%$, $Sp = 94.4\%$, notably outperforming detection based on the ST series in all cases, with the same detector structure. The timing of the detected ischemic events ranged from 30 s up to 150 s (mean = 66.8 s) following the start of occlusion. We conclude that changes in the QRS angles can be used to detect acute myocardial ischemia.

Keywords: QRS angles, PCI, myocardial ischemia, Laplacian noise

(Some figures may appear in colour only in the online journal)

1. Introduction

Ischemia detectors are commonly applied in two scenarios: Holter monitoring, typically during 24 hours, to assess patients with suspected or known coronary artery disease (CAD); and continuous monitoring (e.g. in intensive care units). Most ischemia detectors are based on evaluation of changes in the ST segment deviation of the electrocardiogram (ECG), which has been traditionally considered as the most sensitive marker to diagnose ischemia in clinical practice (Shook *et al* 1987, Taddei *et al* 1995, García *et al* 1998, Jager *et al* 1998, Stadler *et al* 2001, Smrdel and Jager 2004). Because ST segment changes may result from many other causes apart from ischemia, such as variations in the electrical heart axis due to body position changes, heart rate-related events, other electrical conduction changes or ECG artifacts, many ST-based ischemia detectors developed are not robust enough to distinguish between ischemic and non-ischemic episodes of ST segment changes (Mincholé *et al* 2010), which nowadays still remains a challenge.

Other ischemia detectors have also taken into account changes in the T wave morphology and in the entire ST-T complex rather than in the ST segment only (Laguna *et al* 1999, García *et al* 2000a). When ischemia becomes acute, ECG changes are also reflected in the depolarization phase (QRS complex) (Barnhill *et al* 1989, Surawicz 1998, Weston *et al* 2007, Wong *et al* 2009). In particular, QRS duration (Michaelides *et al* 1993, Cantor *et al* 1998), high-frequency QRS components (in the band of 150–250 Hz) (Pettersson *et al* 2000) and QRS slopes (Firoozabadi *et al* 2016, Pueyo *et al* 2008) have been proposed as depolarization markers for detecting induced ischemia, either during stress exercise or coronary occlusion. Thus, depolarization changes could be used to trigger an alert indicating the presence of a more severe ischemia.

In a recent work, temporal and spatial changes in the three QRS angles, shown in figure 1, were characterized during coronary occlusion (Romero *et al* 2013). In that study the R wave angle was found to be correlated with the amount of the image-based quantified ischemia while the other two angles presented a fast transient ischemia-induced change, which suggested they could be appropriate features for ischemia detection. In this work, we present and evaluate a myocardial ischemia detector based on the quantification of these QRS angles, for which a model of gradual transitions with Laplacian additive error is assumed.

2. Materials and methods

2.1. Population

The STAFF III dataset comprised 108 patients admitted to the Charleston Area Medical Center in West Virginia, USA, for prolonged, elective percutaneous coronary intervention (PCI) due to stable angina pectoris (Wagner *et al* 1988, García *et al* 2000b). The following inclusion criteria were met for each patient of this database:

- no clinical or ECG evidence of an acute or recent myocardial infarction,
- no intraventricular conduction delay with QRS duration equal to or more than 120 ms (including left and right bundle branch block),
- no pacemaker rhythm, low voltage, atrial fibrillation/flutter or any irregular ventricular rhythm at inclusion or at the time of the PCI.

Patients undergoing an emergency procedure or presenting signal loss during acquisition were excluded from the original dataset so that a total of 79 patients were included in our study.

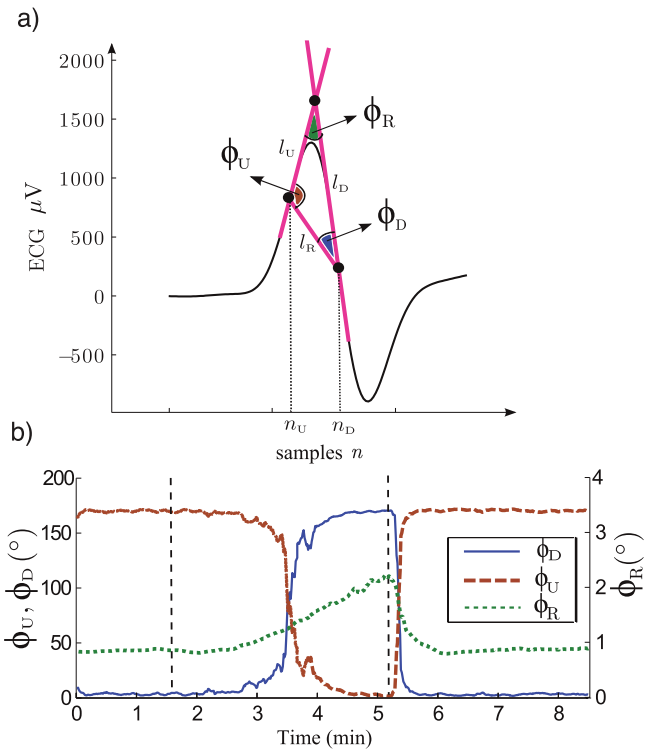

Figure 1. (a) QRS angles evaluated in this study. (b) Temporal evolution of the angles ϕ_U and ϕ_D during coronary occlusion, comprised within the two dashed vertical lines.

All ECGs were recorded using equipment provided by Siemens-Elema AB, Solna, Sweden. Nine standard leads (V1-V6, I, II and III) were recorded and digitized at a sampling rate of 1 kHz with an amplitude resolution of 0.6 μV. The three augmented leads aVL, -aVR and aVF were then generated from the limb leads to yield the complete standard 12-lead ECG system. For each patient, two ECG recordings were acquired. The first one served as a control recording and was continuously acquired in resting supine position for 5 min within the hour prior to the beginning of the PCI procedure. The second one served for ischemia analysis and was continuously acquired during the PCI procedure (from balloon inflation to deflation). The duration of the occlusion ranged from 1 min 30 s to 7 min 17 s (mean 4 min 26 s). The occlusion sites of the PCI procedures were: left anterior descending coronary artery (LAD) in 25 patients, right coronary artery (RCA) in 38 patients and left circumflex coronary artery (LCX) in 16 patients. The electrodes were either retained on the patient between the recordings, or removed but with their positions being marked, to enable accurate comparisons of the ECG variables.

2.2. Preprocessing

All ECG signals involved in the study were preprocessed before evaluation of the analyzed indices as follows: (1) QRS complex detection, (2) selection of normal beats according to Moody and Mark (1982), (3) baseline drift attenuation via cubic spline interpolation and (4) wave delineation using a wavelet-based technique (Martínez *et al* 2004).

2.3. QRS angles evaluated from standard leads

The QRS angles evaluated in this study are illustrated in figure 1. In brief, lines l_U and l_D were obtained by least square fitting the ECG signal in 8-ms windows centered at points of maximal inflection n_U and n_D respectively in the upstroke and downstroke of the ECG around the R wave peak. The line l_R was additionally obtained by connecting the points $[n_U, x(n_U)]$ and $[n_D, x(n_D)]$ where $x(n)$ is the ECG signal. The slopes of the lines l_U, l_D and l_R were denoted by s_U, s_D and s_R respectively. s_U and s_D were obtained from the least square fitting, whereas s_R was calculated as $s_R = \frac{x(n_D) - x(n_U)}{n_D - n_U}$.

The three QRS angles were obtained from the triangle built from the intersection of the lines l_U, l_D and l_R, as shown in figure 1.

- ϕ_U: the up angle of the R wave
- ϕ_D: the down angle of the R wave
- ϕ_R: the R-wave angle

The full methodology used to compute the QRS angles is described in Romero *et al* (2013). The angles ϕ_U, ϕ_R and ϕ_D were calculated in the following order. First, the angle ϕ_R was assumed to be an acute angle ($<90°$) and was calculated using the general angular expression:

$$\phi_R = \arctan\left(\left|\frac{s_U^* - s_D^*}{1 + s_U^* s_D^*}\right|\right) \tag{1}$$

where s_U^* and s_D^* are the slopes expressed in mm/mm. The next step consisted in first computing ϕ_U or ϕ_D depending on the s_R value, as described in Romero *et al* (2013). If the slope s_R was positive, the angle ϕ_U was first computed using an expression analogous to (1) and subsequently the angle ϕ_D was computed as $\phi_D = 180° - (\phi_R + \phi_U)$. Conversely, if the slope s_R was negative, we first computed ϕ_D and then ϕ_U following the same strategy. To compute the expression in (1) time and amplitude were re-scaled to match that of ECG tracings in clinical printouts, where a speed of 25 mm s^{-1} and a gain of 10 mm mV^{-1} are conventionally used. In this way, all the slopes denoted as s^* are expressed in mm/mm for the typical scaling. Depending on the original amplitude resolution as well as the sampling rate of the analyzed ECG signals, the slopes s_U and s_D (in $\mu V\ ms^{-1}$) in the equation for ϕ_R need to be multiplied by a scaling factor to convert from, in this particular case, $\mu V\ ms^{-1}$ to mm/mm (i.e. 1 $\mu V\ ms^{-1}$ = 0.01 mm/0.025 mm = 0.4 mm/mm) resulting in s_U^* and s_D^*. Considering that conversion, (1) can be written as:

$$\phi_R = \arctan\left(\left|\frac{s_U - s_D}{0.4(6.25 + s_U s_D)}\right|\right). \tag{2}$$

The same conversion was also applied to the other two angles, ϕ_U and ϕ_D, by scaling the slopes involved—s_R and s_U in the case of ϕ_U, and s_R and s_D in the case of ϕ_D.

2.4. QRS angles evaluated from transformed leads

In addition to the standard leads, transformed leads were derived from the PCA technique. The transformed leads were obtained by learning from sets of three contiguous leads of the standard system (i.e. V1–V2–V3, V2–V3–V4, ..., II-aVF-III). Then, the transformed lead associated with the first principal component of each set was retained:

$$l_k^{PCA}(n) = \mathbf{u}_k^T \cdot \mathbf{l}_k(n), \qquad k = 1, ..., K. \tag{3}$$

where K is the total number of lead subsets ($K = 10$) and $\mathbf{u}_k$ is the first column of the matrix $\mathbf{U}_k$ (containing the right singular vectors), representing the first principal component obtained after applying singular value decomposition (SVD) of the matrix $\mathbf{L}_k$:

$$\mathbf{L}_k = \mathbf{U}_k \mathbf{\Sigma} \mathbf{V}' \tag{4}$$

which contains the 3 leads of subset k, represented by $\mathbf{l}_k(n)$. With this notation,

$$\mathbf{l}_k(n) = [l_{k,1}(n), l_{k,2}(n), l_{k,3}(n)]^T \tag{5}$$

and

$$\mathbf{L}_k = [\mathbf{l}_k(0), \mathbf{l}_k(1), \ldots, \mathbf{l}_k(N)] \tag{6}$$

where $l_{k,j}(n)$ is the nth sample of the jth lead in subset k, and N denotes the total number of samples.

2.5. Ischemia detection using a GLRT-based method

In Romero *et al* (2013) it is shown that the temporal evolution of the angles ϕ_U and ϕ_D in response to the induced ischemia follows a non-linear pattern, especially in those leads close to the ischemic region, unlike the observed one for ϕ_R, which was much more linear and gradual during the whole occlusion process (figure 1(b)). These observations served to formulate an ischemia detection problem where a step-like pattern with a short transition in ϕ_U and ϕ_D was searched for in a running observation window throughout the PCI recording.

The angle series of ϕ_U or ϕ_D represented here as $\varphi_l[n]$, and computed for each lead l, was considered in determining whether an acute ischemic episode occurred (hypothesis $\mathcal{H}_1$) or only noise was present (hypothesis $\mathcal{H}_0$) in the observation window of length D. The acute ischemic episodes were assumed to be represented by a unitary step with a linear transition $h[n]$, $n = 0, \ldots, D-1$, scaled by a lead-dependent amplitude a_l (see figure 2) and distorted by an additive, lead-dependent noise signal $w_{l[n]}$ with mean value m_l and Laplacian distribution, which can be estimated based on the angles' probability density functions calculated in the control recordings. For the window starting at $n = n_0$, the signal model is:

$$\left.\begin{aligned} &\mathcal{H}_0 : \varphi_l[n] = w_l[n], \\ &\mathcal{H}_1 : \varphi_l[n] = a_l h[n - n_0] + w_l[n]. \end{aligned}\right\} \quad n = n_0, \ldots, n_0 + D - 1 \tag{7}$$

where D represents the length of the observation window (an even-valued integer), and $l = 1$, ..., L represents the lead number. The acute ischemic episodes, of transition duration T (even-valued integer), were modeled as:

$$h[n] = \begin{cases} 1, & n = 0, ..., \dfrac{D-T}{2} - 1 \\ 1 - \dfrac{2}{T+1}\left(n - \dfrac{D-T-2}{2}\right), & n = \dfrac{D-T}{2}, ..., \dfrac{D+T}{2} - 1 \\ -1, & n = \dfrac{D+T}{2}, ..., D-1 \end{cases} \tag{8}$$

The noise $w_{l[n]}$ was assumed to have a Laplacian probability density function (PDF):

$$p(w_l[n]) = \frac{1}{\sqrt{2}\,\sigma_l} \exp\left[-\frac{\sqrt{2}}{\sigma_l} |w_l[n] - m_l| \right] \tag{9}$$

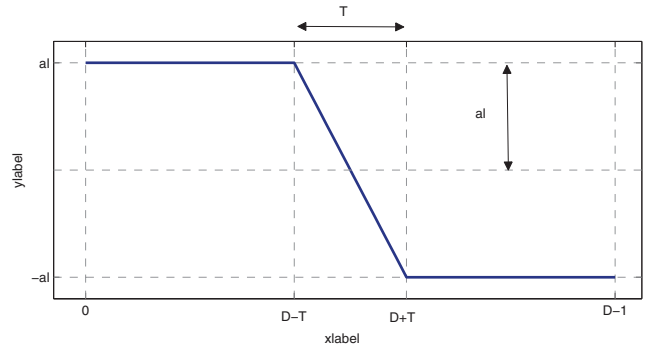

Figure 2. Step-like change with a transition of duration T.

with mean m_l and variance σ_l^2. All variables were assumed to be mutually independent and uncorrelated to the observation angle series $\varphi_l[n]$.

Figure 3 shows the histograms of the noise samples $\hat{w}_l[n]$, resulting from the control recordings of the database in leads V5 and V6. Data corresponding to all patients merged after subtracting the median. All these samples together defined the set Ψ. The notation $\hat{w}_l[n]$ is obtained after subtracting from $w[n]$ its own median in each control and lead, i.e. $\hat{w}_l[n] = w_l[n] - \text{median}(w_l[n])$; the mean was subtracted instead when the Gaussian model was studied. As illustrated in figure 3, the distributions of the angle series have a leptokurtic behavior, being more closely modeled by a Laplacian distribution than by a Gaussian distribution.

$$L_{\text{L}}(\sigma_L; \mathbf{x}_l) = \prod_{n\in\Psi} \frac{1}{\sqrt{2}\,\sigma_l} \exp\left[-\frac{\sqrt{2}}{\sigma_L}\left|\hat{w}_l[n]\right|\right], \tag{10}$$

$$L_{\text{G}}(\sigma_{\text{G}}; \mathbf{x}_l) = \prod_{n\in\Psi} \frac{1}{\sqrt{2\pi\sigma_{\text{G}}^2}} \exp\left[-\frac{\hat{w}_l^2[n]}{2\sigma_{\text{G}}^2}\right]. \tag{11}$$

Moreover, the logarithm of the likelihood values are displayed within each graph, confirming that the Laplacian model is the best fitting model, presenting fewer negative values. Similar observations took place in the remaining leads.

The generalized likelihood ratio test (GLRT), based on the Neyman–Pearson theorem, was used as the basis for ischemia detection. Basically the GLRT is the likelihood ratio between the probabilities associated with the two hypotheses, when the unknown parameters of the signal model, under both hypothesis $\mathcal{H}_0$ and $\mathcal{H}_1$, are replaced with their maximum likelihood estimates (MLEs). Thus, using the Laplacian distribution, the GLRT decides $\mathcal{H}_1$ or $\mathcal{H}_0$ according to:

$$\begin{aligned}\Lambda_{\text{G}}^{n_0}(\boldsymbol{\varphi}_l) &= \frac{p(\boldsymbol{\varphi}_l; \hat{a}_{l,\mathcal{H}_1}, \hat{m}_{l,\mathcal{H}_1}, \mathcal{H}_1)}{p(\boldsymbol{\varphi}_l; \hat{m}_{l,\mathcal{H}_0}, \mathcal{H}_0)} \\ &= \frac{\exp\left[-\dfrac{\sqrt{2}}{\sigma_l}\displaystyle\sum_{n=n_0}^{n_0+D-1}\left|\varphi_l[n] - \hat{m}_{l,\mathcal{H}_1} - \hat{a}_{l,\mathcal{H}_1} h[n-n_0]\right|\right]}{\exp\left[-\dfrac{\sqrt{2}}{\sigma_l}\displaystyle\sum_{n=n_0}^{n_0+D-1}\left|\varphi_l[n] - \hat{m}_{l,\mathcal{H}_0}\right|\right]} \gtrless_{\mathcal{H}_0}^{\mathcal{H}_1} \gamma\end{aligned} \tag{12}$$

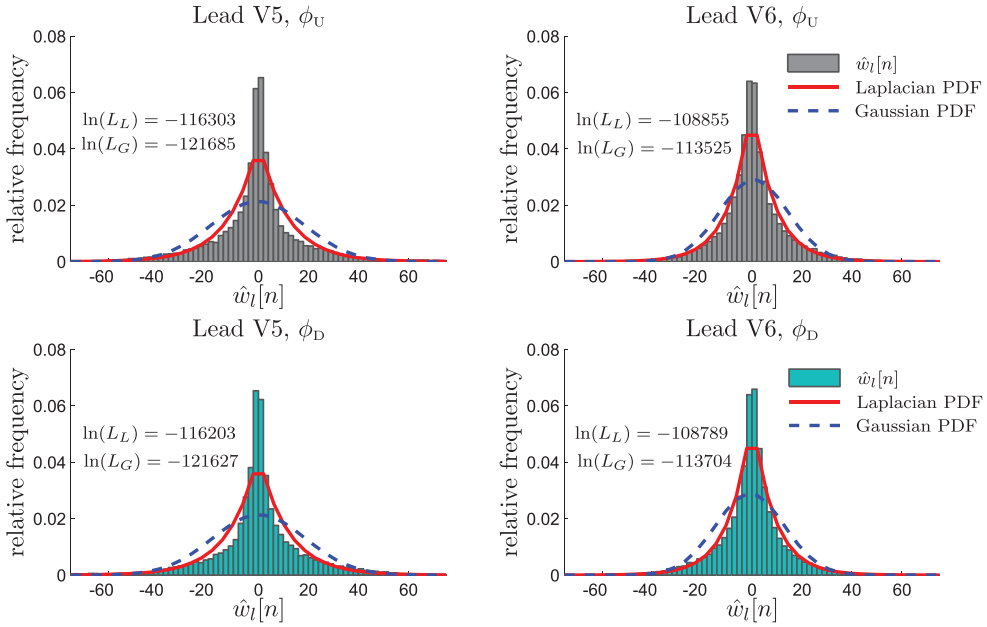

Figure 3. Histograms of $\hat{w}_l[n]$ for ϕ_{U} and ϕ_{D} in leads V5 (left column) and V6 (right column) with the best fit of the Laplacian and Gaussian probability density functions obtained by maximizing their respective likelihood functions. $\ln(L_{\mathrm{L}})$ and $\ln(L_{\mathrm{G}})$ are the values of the log likelihood obtained for each fitting noise model.

where $\hat{a}_{l,\mathcal{H}_i}$ and $\hat{m}_{l,\mathcal{H}_i}$ denote the MLEs of a_l and m_l under hypothesis $\mathcal{H}_i$ ($i = 0, 1$). Vector $\boldsymbol{\varphi}_l$ denotes the vector consisting of the samples $\varphi_l[n]$, $n = n_0, ..., n_0 + D - 1$.

2.6. Calculation of the MLEs $\hat{m}_{l,\mathcal{H}_0}$, $\hat{m}_{l,\mathcal{H}_1}$ and $\hat{a}_{l,\mathcal{H}_1}$

The MLEs $\hat{m}_{l,\mathcal{H}_0}$, $\hat{m}_{l,\mathcal{H}_1}$ and $\hat{a}_{l,\mathcal{H}_1}$ used in the ischemia detector were computed as (see appendix for derivation):

$$\hat{m}_{l,\mathcal{H}_0} = \mathrm{med}(\varphi_l[n]) \tag{13}$$

$$\hat{m}_{l,\mathcal{H}_1} = \mathrm{med}(\varphi_l[n] - \hat{a}_{l,\mathcal{H}_1} h[n - n_0]) \tag{14}$$

$$\hat{a}_{l,\mathcal{H}_1} = \mathrm{med}\left(|h[n - n_0]| \lozenge \left(\frac{\varphi_l[n] - \hat{m}_{l,1}}{h[n - n_0]} \right) \right) \tag{15}$$

where $\mathrm{med}(\alpha_i \lozenge x_i)$ denotes the weighted median (Arce 1998) of x_i with weights α_i and $n = n_0, \ldots, n_0 + D - 1$.

As both MLEs $\hat{m}_{l,\mathcal{H}_1}$ and $\hat{a}_{l,\mathcal{H}_1}$ need to be estimated together, an iterative optimization was applied. An initial estimate $\hat{m}_{l,\mathcal{H}_1}$ was taken as the median of $\varphi_l[n]$, based on the symmetry of $h[n]$ (Mincholé *et al* 2014). This was included in (15) to compute $\hat{a}_{l,\mathcal{H}_1}$. The obtained value was then included back in (14) to compute $\hat{m}_{l,\mathcal{H}_1}$ and so forth until convergence. Typically, stable values for $\hat{m}_{l,\mathcal{H}_1}$ and $\hat{a}_{l,\mathcal{H}_1}$ were achieved in less than 10 iterations.

Considering the MLEs for the unknown parameters ($\hat{m}_{l,\mathcal{H}_0}$, $\hat{m}_{l,\mathcal{H}_1}$ and $\hat{a}_{l,\mathcal{H}_1}$) and applying the logarithm to both sides of (12), we got:

$$
\begin{aligned}
T[n_0] &= \ln \Lambda_{\mathrm{G}}^{n_0}(\boldsymbol{\varphi}_l) \\
&= \frac{\sqrt{2}}{\hat{\sigma}_l} \sum_{n=n_0}^{n_0+D-1} (|\varphi_l[n] - \hat{m}_{l,\mathcal{H}_0}| \\
&\quad -|\varphi_l[n] - \hat{m}_{l,\mathcal{H}_1} - \hat{a}_{l,\mathcal{H}_1} h[n-n_0]|) \underset{\mathcal{H}_0}{\overset{\mathcal{H}_1}{\gtrless}} \gamma'
\end{aligned} \tag{16}
$$

with $\gamma' = \ln\gamma$. The standard deviation (SD) of the Laplacian noise in (16), $\hat{\sigma}_l$, was estimated from an interval containing N_{σ_l} samples corresponding to the entire baseline control recording $\varphi_l^b[n]$:

$$
\hat{\sigma}_l = \frac{\sqrt{2}}{N_{\sigma_l}} \sum_{n=1}^{N_{\sigma_l}} \left| \varphi_l^b[n] - \hat{m}_l^b \right| \tag{17}
$$

where $\hat{m}_l^b$ is the sample median of $\varphi_l^b[n]$. Note that the Gaussian counterpart of the standard deviation is $\hat{\sigma}_l = \frac{1}{N_{\sigma_l}} \sum_{n=1}^{N_{\sigma_l}} (\varphi_l^b[n] - \hat{m}_l^b)^2$.

The detector statistic $T[n_0]$ in (16) can be interpreted as the difference between the mean absolute deviation of the signal and the mean absolute deviation after subtracting the estimated step. Therefore, if the signal does really have a step-like shape, $T[n_0]$ will have a larger value.

A simulated example is illustrated in figure 4. The detector parameters were selected to have values close to the real ones as obtained from the analysis of the QRS angles. The step-like change with linear transition was defined to have an amplitude of $a_l = 50°$ and centered at the time instant $n = 300$. It was then contaminated with an additive Laplacian noise with mean $m_l = 100°$ and SD $\sigma_l = 5°$. Five different time instants were selected to obtain the corresponding detection outputs: well before or nearly before, centered at the timing of the step-like change, just after or well after it. The sliding window duration for the GLRT was set at $D = 100$ s with a transition duration of $T = 20$ s. As illustrated in the bottom panel of figure 4, the detector is quite insensitive to the different tested values for the parameter T as compared with the optimum one $T = 20$ s.

2.7. Design parameters of the ischemia detector

The design of the ischemia detector applied to the QRS angles series is presented in figure 5. It consists of three individual detectors working in parallel, where each one works with a different subset of leads. The final lead subset selected within each individual detector of the two available strategies (standard ECG leads or the first component of PCA-transformed leads, shown above and below the input lines of the detector blocks in figure 4) is that maximizing the detection performance in terms of sensitivity (*Se*) and specificity (*Sp*), when evaluated in the three occluded artery groups. Specifically, the optimal detector was selected based on the computation of the statistic $J = Se + Sp - 1$, known as Youden's index. Note that all the detectors share a common configuration, which is displayed on the right side of figure 5. The procedure applied to determine the optimal parameters of each individual detector as well as the most sensitive lead subset is described below.

2.7.1. GLRT detector block. All QRS angle series evaluated in standard and transformed leads were filtered to remove outliers using a median absolute deviation (MAD) method (Hampel 1987) and were subsequently resampled at 1 Hz.

For the GLRT detector, the duration of the observation window D was set to 70 s. This value was selected considering the smaller occlusion duration in the analyzed database. For the duration T of the transition, different values were tested ranging from 2 to 58 s in 4s

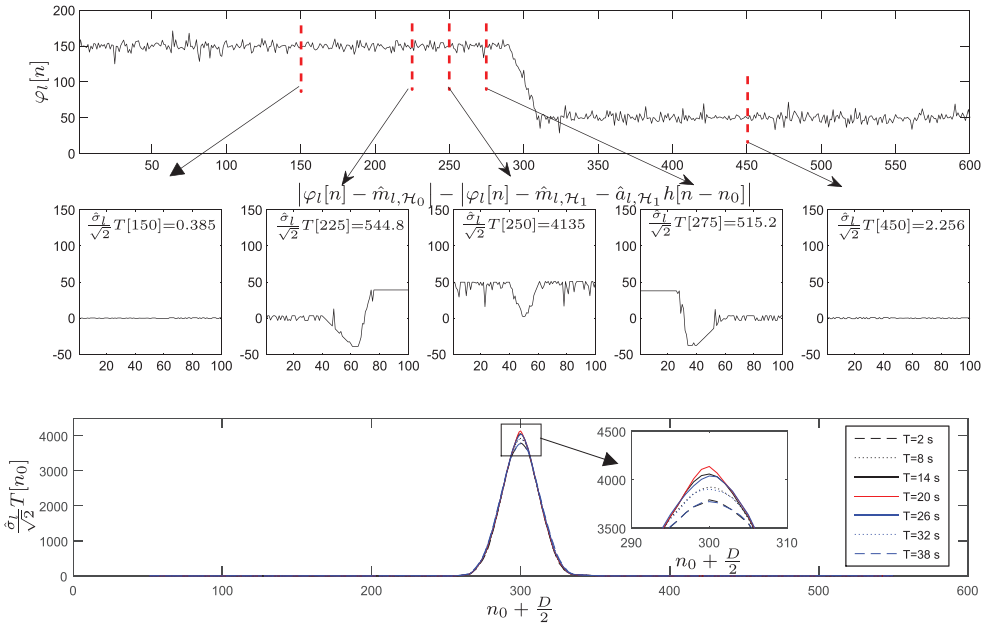

Figure 4. Simulated example of the ischemia detector performance. Evaluation is shown at five different positions marked as dashed red vertical lines superimposed to the series of $\varphi_l[n]$ corresponding to $n_0 = 150, 225, 250, 275, 450$. $\varphi_l[n]$ contains a step-like change with linear transition occurring at $n = 300$. The additive Laplacian noise has a median of $m_l = 100°$ and standard deviation of $\sigma_l = 5°$. The output is displayed for different transition values corresponding to the optimum $T = 20$ s plus three larger and three smaller T values. The duration of the observation window is $D = 100$ s.

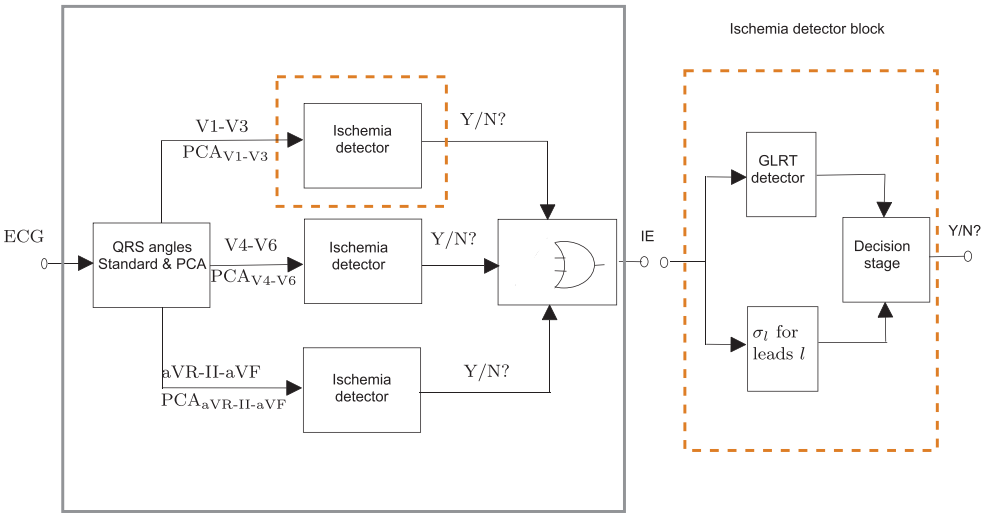

Figure 5. General block-diagram of the ischemia detector design. The block on the right side represents the internal configuration of each ischemia detector block for the analyzed leads l corresponding to either three standard leads or a PCA-transformed lead. IE: ischemic episode.

steps to cover the different transition durations observed in the analyzed recordings. The QRS angles ϕ_U and ϕ_D were independently considered in the detection process using (16).

2.7.2. Noise estimation. The estimates $\hat{\sigma}_l$ in (17) were obtained for each analyzed lead l from the control recording of each patient. This implies that, even when the signal amplitude is very similar between leads, the detector statistic will be adapted to the noise level in each individual lead. Therefore, the individual detector outputs corresponding to the leads involved were independently used to apply the final decision in case of using the standard leads separately. When using the PCA transformed leads, only the detector output corresponding to the first principal component was taken into account.

2.7.3. Decision stage. After lead selection (applied in the cases of standard leads only), a lead-dependent threshold γ'_l for the detector statistic was selected as a function of the SD $\hat{\sigma}_l$ and the window length D: $\gamma'_l = \delta\sigma_l D$, where different values of δ were tested. In the case of using standard ECG leads the threshold γ'_l was required to be exceeded by at least one of the three detector outputs (corresponding to the three leads involved) to consider the detection of an ischemic event. In the case of using a PCA-transformed lead, a threshold γ'_l was fixed for the corresponding detector output. Figure 6 displays an example with the outputs of the four individual ischemia detectors (figure 6(b)) applied over the series of the angle ϕ_U in four (figure 6(a)) precordial leads (V2–V5) for a particular recording corresponding to a LAD occlusion. The value of δ was set to 8 whereas the transition T was set to either $T = 20$ or $T = 40$ s. It can be observed that two successful detections took place (leads V2 and V3) and two others failed (leads V4 and V5).

2.7.4. Performance evaluation. To evaluate the performance of the proposed ischemia detector, *Se* and *Sp* were computed. All the PCI recordings were considered to have ischemia while all the control recordings were considered not to have ischemia. The performance was individually assessed for each group of patients according to the occlusion site. The *Se* and *Sp* values were evaluated for different thresholds γ' (as a function of δ, $\delta = 0.01, 0.02, ..., 40$) and transition durations T (ranging between 2 and 58 s) in the ischemia detector. The optimal values of γ' and T maximizing the detection performance according to Youden's index were selected for the final ischemia detector.

In order to evaluate the performance of the QRS angle-based detector described above as compared to an ST-based detector, *Se* and *Sp* were additionally evaluated after applying the same ischemia detector to the ST series, calculated as the ST level measured at J point plus 60 ms.

2.8. Timing of ischemic episodes

The time t_E elapsed from the beginning of the occlusion, t_0, until the instant when an ischemic event was detected, t_{IE}, was also evaluated ($t_E = t_{IE} - t_0$) for each patient. Because ischemic events were detected at different time instants depending on the analyzed lead, we considered the estimated detection time as corresponding to the earliest time when any detection statistic was above the corresponding threshold (see figure 6).

2.9. Dynamics of the QRS angles

As the proposed ischemia detector was tested in PCI, recordings presenting a clear change in QRS angles and additional control recordings were available; we quantified and characterized the values of the QRS angles at baseline and just before the end of the balloon inflation,

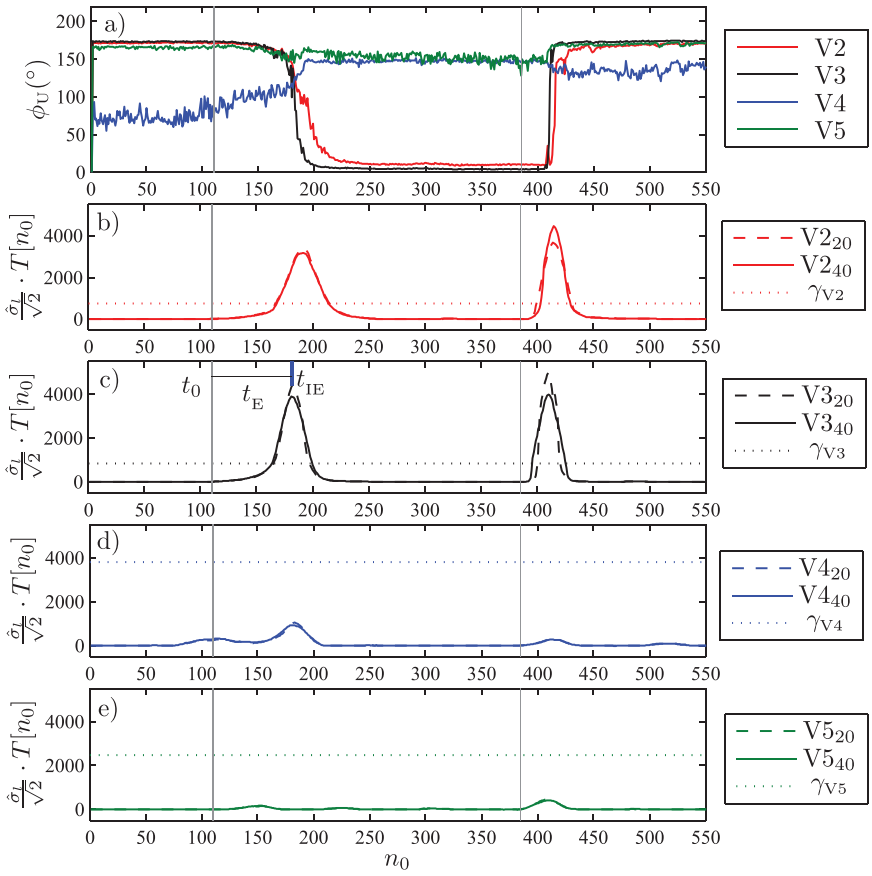

Figure 6. Example of how the ischemia detector works on a recording of a patient with LAD occlusion: (a) ϕ_U series corresponding to leads V2–V5; (b) ischemia detector outputs corresponding to lead V2, (c) lead V3, (d) lead V4 and (e) lead V5. Two values for parameter T ($T = 20$ and $T = 40$ s) are shown. Horizontal dashed lines correspond to thresholds obtained by using $\delta = 8$ in the computation of γ'_l for each lead. Vertical gray lines mark the occlusion period. Vertical blue line marks the earliest time instant related to the detected ischemic event.

corresponding to maximum changes. These values were statistically compared. Statistical analysis was carried out for the whole population and for each of the three artery groups using the nonparametric Wilcoxon signed-rank test. The significance level was defined as $p < 0.05$.

3. Results

3.1. Ischemia detection using PCA-transformed ECG leads

The performance of the ischemia detector was evaluated in transformed leads obtained from PCA. Figure 7 shows the ROC curves corresponding to three different transition values T ($T = 2$, 26, 58 s) evaluated for different thresholds γ' (obtained with $\delta = 0.01, 0.02, ..., 40$). Results in figure 7 correspond to the angle ϕ_U evaluated in PCA transformed leads generated from leads V1–V3 (LAD group, left panel) and aVR-II-aVF (RCA group, right panel). The optimal values for parameters δ and T are those simultaneously maximizing *Se* and *Sp*,

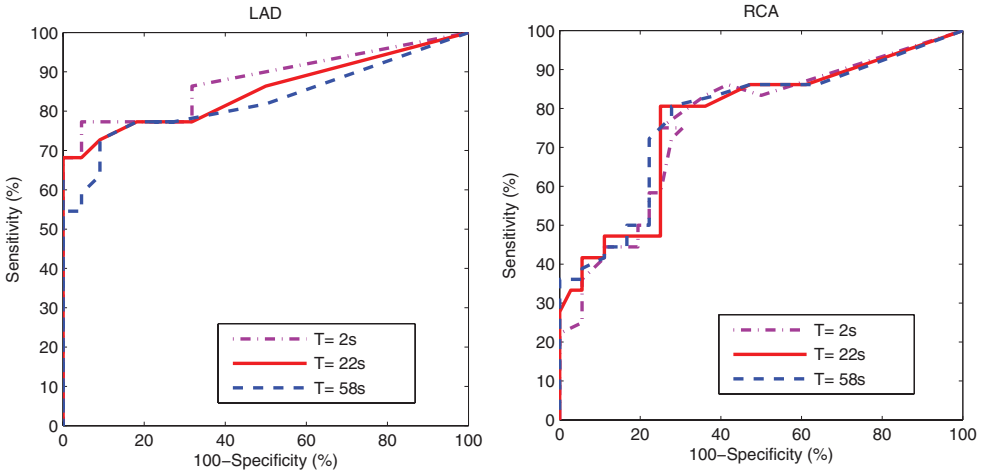

Figure 7. Receiver operating characteristic curves obtained for different transition values T and evaluated for different thresholds γ' in the LAD group (left) and RCA group (right) for the angle ϕ_{U}.

i.e. the closest point to the left-top corner in the ROC curve. From the figure it is clear that all tested T values yield similar results. The two PCA-transformed leads with the best performance in terms of their area-under-the-curve (AUC) values are summarized in table 1, for both ϕ_{U} and ϕ_{D} angles and each of the three artery groups. The corresponding *Se* and *Sp* values are also shown in each case.

The LAD group presented the highest global detection performance when comparing the resulting AUCs, achieving a maximum value of 87.7%, whereas values for RCA and LCX groups were 78.4% and 78.5% respectively.

3.2. Ischemia detection using standard ECG leads

The performance of the ischemia detector was also tested in standard ECG leads. As previously described in section 2.7.3, an ischemic event was considered as detected if any of the leads involved in the combination of standard leads met the specified criterion. Results are summarized in table 2 for the three artery groups and for the two lead combinations with the best detection performance. The two QRS angles ϕ_{U} and ϕ_{D} yield similar performance. Precordial leads V1-V3 presented the best results in the LAD group and led to a global performance in terms of AUC of 93.1%. In the RCA group, leads aVR, II and aVF were the best suited for ischemia detection and reached a global performance of 91.2%. In the LCX group leads V4-V6 were the ones with the highest detection capability, achieving an AUC of 95.8%. Figure 8 shows the ROC curves obtained for the RCA group using the two optimal lead combinations and a range of T values.

The optimal δ value obtained in each artery group was highly dependent on the range of changes in the ϕ_{U} and ϕ_{D} angles developed during the occlusion as well as the respective SD values measured in control. For the LAD group, the optimal δ value was $\delta = 2.4$; for the RCA group, $\delta = 0.35$; and for the LCX group, $\delta = 0.14$.

Table 2 also shows results obtained when applying the ischemia detector to the ST level series. It can be observed that, using the same sets of leads, the QRS angles notably outperform the results obtained with the ST segment.

Table 1. Optimal ischemia detector's performance using PCA-derived leads.

QRS Angle	LAD *Se*/*Sp*(%) AUC	RCA *Se*/*Sp*(%) AUC	LCX *Se*/*Sp*(%) AUC
	V1–V3	aVR-II-aVF	V4–V6
Angle ϕ_U	77.3/95.5	83.3/72.2	72.2/77.8
	87.7	78.4	78.5
Angle ϕ_D	77.3/100	75.0/77.7	66.7/66.7
	82.9	77.0	72.1
	V2–V4	II-aVF-III	V5–V6-aVL
Angle ϕ_D	72.7/100	47.2/91.6	55.6/100.0
	82.3	67.7	77.5
Angle ϕ_U	77.3/100	36.1/100	61.1/94.4
	84.7	72.4	75.5

Table 2. Optimal ischemia detector's performance using combinations of standard ECG leads.

QRS angles/ ST level	LAD *Se*/*Sp*(%) AUC	RCA *Se*/*Sp*(%) AUC	LCX *Se*/*Sp*(%) AUC
(Lead comb.)	(V1–V3)	(aVR-II-aVF)	(V4–V6)
ϕ_U	86.4/100	86.1/94.4	88.9/88.9
	91.5	91.2	88.9
ϕ_D	90.9/95.4	86.1/91.7	88.9/94.4
	93.1	90.3	95.8
ST_{60}	77.7/85.2	76.3/97.7	44.4/72.7
	80.1	87.5	59.8
(Lead comb.)	(V2–V4)	(II-aVF-III)	(V5–V6-aVL)
ϕ_U	81.8/100	86.1/91.7	66.7/100
	89.2	89.8	90.6
ϕ_D	86.4/96.3	80.6/94.4	94.4/66.7
	90.9	88.9	88.1
ST_{60}	77.4/82.6	77.3/100	77.8/87.5
	78.1	86.2	81.6

3.3. Timing of ischemic events

The timing of detected ischemic events with respect to the beginning of the occlusion was 66.8 ± 30.9 s for the whole study population. Particularizing for the LAD group, the timing was 72.3 ± 29.8 s (range: 27–88 s); in the RCA group, 71.9 ± 33.3 s (range: 27–154 s); and in the LCX group, 46.6 ± 22.2 s (range: 31–122 s). The above results indicate that in some patients ischemia can be detected as a change in the QRS angles as early as 0.5 min after the start of the coronary occlusion, while in others 2.5 min of occlusion are needed.

3.4. Significance of ischemia-induced changes in QRS angles

The averaged values of the QRS angles representative of both baseline (reference) and occlusion stages were computed for each analyzed lead. Although there were significant differences

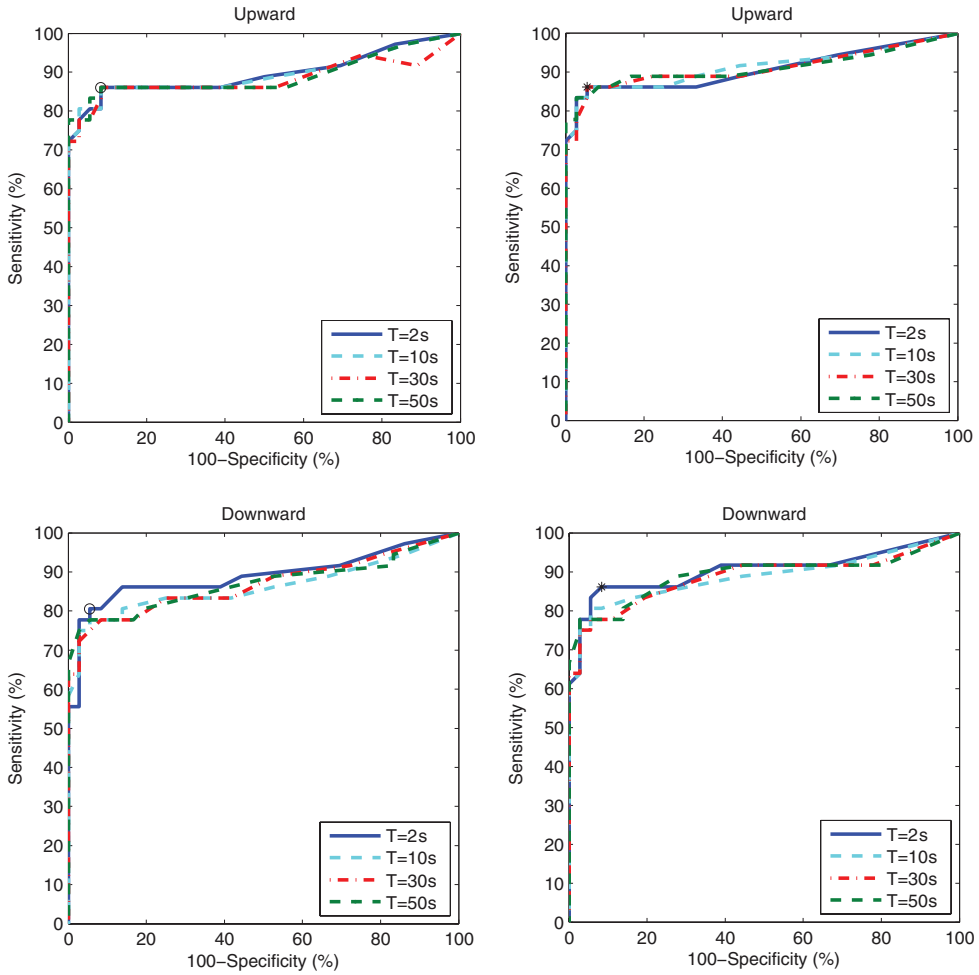

Figure 8. Receiver operating characteristic curves obtained for the RCA group using combinations of standard ECG leads. Left column: using the lead combination II-aVF-III and four different transition durations ($T = 2$, 10, 30, 50 s). Right column: using the lead combination aVR-II-aVF and the same T values.

between these stages in the overall population (especially in precordial leads V2–V5, $p < 0.05$), the most significant differences were observed when comparing these two stages in the LAD group. The largest differences in LAD correspond to leads V2–V4 ($p < 0.001$ in most cases), while in other leads no significant differences were observed. In the RCA group, significant differences were found in leads aVR, II, aVF and III ($p < 0.01$ in all cases). In the LCX group, variations were smaller and only significant in V2 ($p = 0.022$) and V3 ($p = 0.031$). A summary of the QRS angle values before and after coronary occlusion are shown in table 3 for those leads with the greatest differences.

4. Discussion

In this work an acute ischemia detector based on the analysis of the QRS angles, denoted as ϕ_{U} and ϕ_{D}, has been developed and evaluated. The detector was implemented based on a model of Laplacian noise added to a step-like change with a linear transition, modeling the observed

Table 3. Mean ± SD of the QRS angles at baseline and during coronary occlusion.

cc	Angle	$\phi_U(^\circ)$ Baseline ⇒ Ischemia	$\phi_D(^\circ)$ Baseline ⇒ Ischemia
L	V2	140 ± 51 ⇒ 86 ± 67	30 ± 51 ⇒ 75 ± 63
A	V3	147 ± 50 ⇒ 72 ± 65	26 ± 47 ⇒ 96 ± 64
D	V4	154 ± 19 ⇒ 89 ± 65	19 ± 18 ⇒ 83 ± 63
R	II	69 ± 52 ⇒ 53 ± 49	102 ± 53 ⇒ 118 ± 50
C	aVF	60 ± 44 ⇒ 43 ± 39	106 ± 48 ⇒ 121 ± 43
A	III	62 ± 49 ⇒ 39 ± 37	99 ± 153 ⇒ 120 ± 44
L	V5	107 ± 37 ⇒ 85 ± 52	67 ± 38 ⇒ 89 ± 53
C	V6	58 ± 45 ⇒ 46 ± 41	114 ± 48 ⇒ 124 ± 41
X	I	97 ± 36 ⇒ 87 ± 38	62 ± 37 ⇒ 62 ± 43

signature of the QRS angle series during acute ischemia. The QRS angles were previously studied in Romero *et al* (2013) for predicting the extent and severity of ischemia and were found to be very sensitive to the ischemia-induced changes, presenting both ϕ_U and ϕ_D—a sudden change—during coronary occlusion, unlike the gradual changes observed in ϕ_R. The latter turned out to be the best angle in that study for predicting the extension and severity of ischemia, since it reflects concomitant changes occurring in the upstroke and downstroke of the QRS complex, thus providing, in a certain way, a measure of the conduction velocity and a surrogate of the QRS width. On the other hand, the more abrupt changes observed in ϕ_U and ϕ_D occurred several seconds after the occlusion started, changing very quickly up to a certain saturating value reached before occlusion completion. Changes in the angle ϕ_D during occlusion are mainly associated with the non-linear changes occurring in its vertex position (point $[n_D\, x(n_D)]$), produced by the first signs of the induced ischemia, reflected as ST segment elevation or depression depending on the lead, or changes in the S wave. The change in ϕ_D is then inversely reflected in a change of similar magnitude in the angle ϕ_U, except for the smaller changes occurring in ϕ_R. This particular behavior of the angles ϕ_U and ϕ_D has been exploited in this study as a trigger for detecting acute ischemic episodes.

The QRS angles were first evaluated in a set of transformed leads derived from PCA. Different combinations of contiguous standard ECG leads were explored and used to generate the transformed leads. The transformed leads with the highest sensitivity and specificity for ischemia detection were those involving leads close to the region irrigated by the occluded artery. This result is in line with Romero *et al* (2013), where we showed that the standard leads presenting the largest changes in QRS angles during ischemia were those close to the ischemic region.

Although the LAD group developed the largest changes in response to the induced ischemia as a result of the largest irrigated area, the sensitivity of the detector was very similar for the three artery groups, while the specificity was notably higher for LAD. In the RCA and LCX groups, the optimal *Se*/*Sp* values according to Youden's index (J) were of 83.3%/72.2% and 72.2%/77.8% respectively, whereas in the LAD group they were 77.3%/100%. Nevertheless, it is important to highlight that these results were obtained using different thresholds for each group due to the different magnitude of changes developed in each case. In this respect, if a fixed value was to be used for all leads, either higher false positives detection rate for LAD artery or missdetection for RCA and LCX arteries would occur. However, given the different set of leads optimized for each artery occlusion, one can imagine three detectors working in parallel for each potential occluded artery generating ischemia; then each detector could have its own optimum design parameters.

When the ischemia detector was evaluated in standard ECG leads, the detection performance improved with respect to that obtained for PCA-derived leads. In the LAD group the global detection performance in terms of AUC increased from 87.7 to 93.1 (5.4), in RCA from 78.4 to 91.2 (12.8) and in LCX from 78.5 to 95.8 (17.3). The location of the leads associated with the best performance were, nevertheless, the same in the case of the standard and PCA-derived leads. In general, small differences between the outcomes for the two angles, ϕ_U and ϕ_D, were observed, the angle ϕ_U being usually the most sensitive one, especially when evaluated in PCA-transformed leads.

The detection performance of the QRS angles was also compared with that of ST level, by applying the ischemia detector to the series of ST levels. Results shown in table 2 indicate that the sensitivity and specificity values were mostly lower for the ST level, which could to a certain extent be expected due to the more gradual changes occurring in the ST segment during the occlusion period. These values, however, need to be taken in the context of this detector's focus on abrupt changes, since other ST-based detectors, designed for the more gradual ST changes (Jager *et al* 1998), could report better ST-based sensitivity and specificity.

The timing of ischemic episodes was found to be, on average, about one minute after the start of occlusion, starting from only 30 s in some patients up to 150 s for others. This suggests a potential application in which QRS angles could contribute to detection of ischemia and provide an estimate of the occlusion timing as an aid in making decisions regarding therapy to be employed. On the other hand, sudden ischemic changes detected by the proposed detector using the QRS angles series could also serve to distinguish between supply ischemia (eventually given by total artery occlusion) or a more gradual demand ischemia (eventually given by an increased demand associated with heart rate changes and hypothesized to have a much more gradual signature not so easily detectable by this QRS angle-based detector). As both types of ischemic episodes present similar ST patterns (normally gradual transient ST changes rather than sudden changes), the use of QRS angles could help in distinguishing between these situations (Mincholé *et al* 2007). Furthermore, despite not having been considered in this work, the proposed ischemia detector could also be used for detecting the sudden changes occurring after balloon release, which are usually faster and more abrupt than those observed during ischemia onset. Those detections could be useful, for instance, to identify when a clot has been dissolved or removed.

We also assessed the QRS angle values at baseline (in the control recordings) and at the end of artery occlusion (in the PCI recordings) and statistically compared these values. Results showed significant differences between both conditions in the three artery groups, with the greatest differences found in the LAD group. The angle ϕ_u was found to decrease during ischemia, while the opposite was observed for the angle ϕ_d. As discussed above, the QRS angles not only have potential for detecting acute ischemic events, but could also serve to diagnose an existing ischemia, by comparing the current QRS angle values with some reference value, if available, for instance from previous ECG recordings.

Finally, with respect to the design parameters of the detector, we found that detector performance was almost insensitive to the values of parameter T, representing the transition duration of the ischemic change. However, the set of leads involved was a determinant factor when detecting a particular occluded artery. Also, the performance was good for a wide range of values of δ, this being a factor in the definition of the threshold on the detector statistic.

4.1. Limitations of the study

Despite the benefits offered by the proposed detector, there are some limitations that affect its optimum performance. First, the change in the QRS angle series needs to be fast enough

for the statistical model to capture it. The faster the change, the narrower and higher the peak in the detector output, thus allowing a more robust and trustworthy detection of the ischemic events. Likewise, the larger the amplitude of the change, the more easily it will be detected. Second, the threshold used to detect the ischemic events varies for LAD, RCA and LCX occlusions, with the resulting need to use parameter values optimized for each one of the internal ischemia detector blocks according to the artery rather than just a single value for all individual blocks; even this limitation can be overcome by having three detectors working in parallel. Furthermore, the design of the ischemia detector was fitted to the particular features of the analyzed database, where the sudden balloon inflation causes a sudden change in the QRS angles, thus, an overfitting effect to the database can be present in the optimized design parameters. It would be desirable to test the proposed ischemia detector in other databases containing more gradual ischemic events, such as the long term ST database (LTSTDB) (Jager *et al* 2003) and the European ST-T Database (Taddei *et al* 1992), to assess improvements in the specificity for the identification of ischemic events.

5. Conclusion

Morphological ECG changes occurring during acute myocardial ischemia, evaluated in this study through a QRS angle-based method, have proved to be a suitable tool to detect acute ischemic episodes. The upstroke and downstroke QRS angles allow detection of more than 85% of acute ischemic events in any of the three major coronary arteries.

Acknowledgments

This work was supported by projects TEC2013-42140-R and TIN2013-41998-R from the Spanish Ministry of Economy and Competitiveness (MINECO), Spain, by Aragón govern and European Social Fund (FSE) under consolidated group BSICoS. EP acknowledges the financial support of Ramón y Cajal program from MINECO, Spain. The computation was performed by the ICTS NANBIOSIS, more specifically by the High Performance Computing Unit of the CIBER in Bioengineering, Biomaterials and Nanomedicine (CIBER-BBN) at the University of Zaragoza.

Appendix

The three MLEs, $\hat{m}_{l,\mathcal{H}_0}$, $\hat{m}_{l,\mathcal{H}_1}$ and $\hat{a}_{l,\mathcal{H}_1}$, needed for computation of the GLRT detector in (16) were computed as follows. Under hypothesis $\mathcal{H}_0$, the MLE of $m_{l,\mathcal{H}_0}$ was found by maximizing the related log-likelihood function of the Laplacian noise model (9) with respect to m_l:

$$\hat{m}_{l,\mathcal{H}_0} = \arg\max_{m_l} \ln p(\boldsymbol{\varphi}_l; m_l) \tag{A.1}$$

which is equivalent to minimizing the cost function:

$$J(m_l) = \sum_{n=n_0}^{n_0+D-1} \left|\varphi_l[n] - m_l\right| \tag{A.2}$$

with derivative:

$$\frac{\partial J(m_l)}{\partial m_l} = -\sum_{n=n_0}^{n_0+D-1} \operatorname{sgn}(\varphi_l[n] - m_l) \tag{A.3}$$

In (A.2) the minimum is reached when m_l takes the median value of the observed data:

$$\hat{m}_{l,\mathcal{H}_0} = \text{med}(\varphi_l[n]) \tag{A.4}$$

Under hypothesis $\mathcal{H}_1$, the MLEs of $m_{l,\mathcal{H}_1}$ and $a_{l,\mathcal{H}_1}$ were determined by maximizing:

$$[\hat{m}_{l,\mathcal{H}_1}, \hat{a}_{l,\mathcal{H}_1}] = \arg\max_{m_l,a_l} \ln p(\boldsymbol{\varphi}_l; m_l, a_l) \tag{A.5}$$

or, equivalently, by minimizing the cost function:

$$J(m_l, a_l) = \sum_{n=n_0}^{n_0+D-1} \left|\varphi_l[n] - m_l - a_l \cdot h[n-n_0]\right| \tag{A.6}$$

with respect to m_l and a_l, respectively. The partial derivative of $J(m_l, a_l)$ with respect to m_l is:

$$\frac{\partial J(m_l, a_l)}{\partial m_l} = -\sum_{n=n_0}^{n_0+D-1} \text{sgn}(\varphi_l[n] - m_l - a_l \cdot h[n-n_0]) \tag{A.7}$$

which, when set to zero, yielded the following MLE:

$$\hat{m}_{l,\mathcal{H}_1} = \text{med}(\varphi_l[n] - \hat{a}_{l,\mathcal{H}_1} h[n-n_0]) \tag{A.8}$$

with $n = n_0, \cdots, n_0 + D - 1$. The partial derivative of $J(m_l, a_l)$ with respect to a_l is:

$$\frac{\partial J(m_l, a_l)}{\partial a_l} = \sum_{n=n_0}^{n_0+D-1} h[n-n_0]\text{sgn}(\varphi_l[n] - m_l - a_l \cdot h[n-n_0]) \tag{A.9}$$

Inserting the definition of $h[n]$ (8) in the above equation:

$$\begin{aligned}\frac{\partial J(m_l, a_l)}{\partial a_l} = &-\sum_{n=n_0}^{n_0+D/2-1} h[n-n_0]\,\text{sgn}(\varphi_l[n] - m_l - a_l \cdot h[n-n_0]) \\ &-\sum_{n=n_0+D/2}^{n_0+D-1} -h[n-n_0] \cdot \text{sgn}(-\varphi_l[n] + m_l - a_l(-h[n-n_0])) \end{aligned} \tag{A.10}$$

$$= -\sum_{n=n_0}^{n_0+D-1} |h[n-n_0]| \cdot \text{sgn}\left(\frac{\varphi_l[n] - m_l}{h[n-n_0]} - a_l\right) \tag{A.11}$$

The MLE of $a_{l,\mathcal{H}_1}$ can be obtained by computing the weighted median:

$$\hat{a}_{l,\mathcal{H}_1} = \text{med}\left(|h[n-n_0]| \lozenge \left(\frac{\varphi_l[n] - m_l}{h[n-n_0]}\right)\right) \tag{A.12}$$

being $n = n_0, \cdots, n_0 + D - 1$ and where $\text{med}\{\cdot \lozenge \cdot\}$ denotes the weighted median operation. The weighted median was computed using the algorithm described in Arce (1998).

An approximate and computationally faster solution to the MLE of $a_{l,\mathcal{H}_1}$ can be given by the expression in (A.13), as the internal part of the sign function in (A.11) under hypothesis $\mathcal{H}_1$ is equal to $\frac{(w_l[n] - m_l)}{h[n-n_0]}$, whose sign is uncorrelated to $|h[n-n_0]|$ which is symmetric:

$$\hat{a}_{l,\mathcal{H}_1} = \text{med}\left(\frac{\varphi_l[n] - m_l}{h[n-n_0]}\right) \tag{A.13}$$

Finally, it should be noted that the MLEs of $m_{l,\mathcal{H}_1}$ and $a_{l,\mathcal{H}_1}$ are dependent on each other, and therefore an iterative optimization algorithm was applied for the computation, as described in the main text.

References

Arce G R 1998 A general weighted median filter structure admitting negative weights *IEEE Trans. Signal Process.* **46** 3195–205

Barnhill J E, Tendera M, Cade H, Campbell W B and Smith R F 1989 Depolarization changes early in the course of myocardial infarction: significance of changes in the terminal portion of the QRS complex *J. Am. Coll. Cardiol.* **14** 143–9

Cantor A, Goldfarb B, Aszodi A and Battler A 1998 Ischemia detection after myocardial infarction: diagnostic value of exercise-induced QRS duration changes evaluated by a new computerized method *J. Electrocardiol.* **31** 9–15

Firoozabadi R, Gregg R E and Babaeizadeh S 2016 Identification of exercise-induced ischemia using QRS slopes *J. Electrocardiol.* **49** 55–9

García J, Lander P, Sörnmo L, Olmos S, Wagner G and Laguna P 1998 Comparative study of local and Karhunen–Loève-based ST-T indexes in recordings from human subjects with induced myocardial ischemia *Comput. Biomed. Res.* **31** 271–92

García J, Sörnmo L, Olmos S and Laguna P 2000a Automatic detection of ST-T complex changes on the ECG using filtered RMS difference series: application to ambulatory ischemia monitoring *IEEE Trans. Biomed. Eng.* **47** 1195–201

García J, Wagner G, Sörnmo L, Olmos S, Lander P and Laguna P 2000b Temporal evolution of traditional versus transformed ECG-based indexes in patients with induced myocardial ischemia *J. Electrocardiol.* **33** 37–47

Hampel F 1987 Robust statistics *Probability and Mathematical Statistics* (New York: Wiley)

Jager F, Moody G B and Mark R G 1998 Detection of transient ST segment episodes during ambulatory ECG monitoring *Comput. Biomed. Res.* **31** 305–22

Jager F, Taddei A, Moody G B, Emdin M, Antolič G, Dorn R, Smrdel A, Marchesi C and Mark R G 2003 Long-term ST database: a reference for the development and evaluation of automated ischaemia detectors and for the study of the dynamics of myocardial ischaemia *Med. Biol. Eng. Comput.* **41** 172–82

Laguna P, Moody G B, García J, Goldberger A and Mark R 1999 Analysis of the ST-T complex of the electrocardiogram using the Karhunen–Loève transform: adaptive monitoring and alternans detection *Med. Biol. Eng. Comput.* **37** 175–89

Martínez J P, Almeida R, Olmos S, Rocha A P and Laguna P 2004 A wavelet-based ECG delineator: evaluation on standard databases *IEEE Trans. Biomed. Eng.* **51** 570–81

Michaelides A, Ryan J M, VanFossen D, Pozderac R and Boudoulas H 1993 Exercise-induced QRS prolongation in patients with coronary artery disease: a marker of myocardial ischemia *Am. Heart J.* **126** 1320–5

Mincholé A, Jager F and Laguna P 2007 Discrimination between demand and supply ischemia episodes in Holter recordings *29th Annual Int. Conf. of the IEEE Engineering in Medicine and Biology Society* pp 2579–82

Mincholé A, Jager F and Laguna P 2010 Discrimination between ischemic and artifactual ST segment events in Holter recordings *Biomed. Signal Process. Control* **5** 21–31

Mincholé A, Sörnmo L and Laguna P 2014 Detection of body position changes from the ECG using a Laplacian noise model *Biomed. Signal Process. Control* **14** 189–96

Moody G B and Mark R G 1982 Development and evaluation of a 2-lead ECG analysis program *Comput. Cardiol.* **9** 39–44

Pettersson J, Pahlm O, Carro E, Edenbrandt L, Ringborn M, Sörnmo L, Warren S G and Wagner G S 2000 Changes in high-frequency QRS components are more sensitive than ST—segment deviation for detecting acute coronary artery occlusion *J. Am. Coll. Cardiol.* **36** 1827–34

Pueyo E, Sörnmo L and Laguna P 2008 QRS slopes for detection and characterization of myocardial ischemia *IEEE Trans. Biomed. Eng.* **55** 468–77

Romero D, Ringborn M, Laguna P and Pueyo E 2013 Detection and quantification of acute myocardial ischemia by morphologic evaluation of QRS changes by an angle-based method *J. Electrocardiol.* **46** 204–14

Shook T L, Valvo V, Hubelbank M, Feldman C L, Stone P H and Ripley K 1987 Validation of a new algorithm for detection and quantification of ischemic ST segment changes during ambulatory electrocardiography *Comput. Cardiol.* **14** 57–62

Smrdel A and Jager F 2004 Automated detection of transient ST—segment episodes in 24 h electrocardiograms *Med. Biol. Eng. Comput.* **42** 303–11

Stadler R W, Lu S N, Nelson S D and Stylos L 2001 A real-time ST—segment monitoring algorithm for implantable devices *J. Electrocardiol.* **34** 119–26

Surawicz B 1998 Reversible QRS changes during acute myocardial ischemia *J. Electrocardiol.* **31** 209–20

Taddei A, Costantino G, Silipo R, Emdin M and Marchesi C 1995 A system for the detection of ischemic episodes in ambulatory ECG *Computers in Cardiology IEEE* pp 705–8

Taddei A, Distante G, Emdin M, Pisani P, Moody G, Zeelenberg C and Marchesi C 1992 The European ST–T database: standard for evaluating systems for the analysis of ST–T changes in ambulatory electrocardiography *Eur. Heart J.* **13** 1164–72 (PMID: 1396824)

Wagner N B, Sevilla D C, Krucoff M W, Lee K L, Pieper K S, Kent K K, Bottner R K, Selvester R H and Wagner G S 1988 Transient alterations of the QRS complex and ST segment during percutaneous transluminal balloon angioplasty of the left anterior descending coronary artery *Am. J. Cardiol.* **62** 1038–42

Weston P, Johanson P, Schwartz L M, Maynard C, Jennings R B and Wagner G S 2007 The value of both ST-segment and QRS complex changes during acute coronary occlusion for prediction of reperfusion-induced myocardial salvage in a canine model *J. Electrocardiol.* **40** 18–25

Wong C K, Gao W, Stewart R A H, French J K, Aylward P E and White H D 2009 Relationship of QRS duration at baseline and changes over 60 min after fibrinolysis to 30 d mortality with different locations of ST elevation myocardial infarction: results from the hirulog and early reperfusion or occlusion-2 trial *Heart* **95** 276–82